Generalized analytical description of relativistic strong-field ionization

Michael Klaiber,* Karen Z. Hatsagortsyan,† and Christoph H. Keitel
Max-Planck-Institut für Kernphysik, Saupfercheckweg 1, 69117 Heidelberg, Germany

(Received 17 March 2024; accepted 9 July 2024; published 5 August 2024)

A relativistic analytical theory of strong-field ionization applicable across the regimes of deep tunneling up to over-the-barrier ionization (OTBI) is developed, accounting also for the bound-state polarization and the Stark shift beyond perturbation theory. The latter improvement with respect to the state-of-the-art quasiclassical theory of Perelomov-Popov-Terent'ev (PPT) for strong-field ionization is essential to describe analytically the ionization in the OTBI regime and to resolve the order-of-magnitude discrepancy of the ionization yield in the relativistic regime with respect to PPT theory that has remained unexplained since the numerical result using the Klein-Gordon equation of Hafizi *et al.* [Phys. Rev. Lett. **118**, 133201 (2017)]. The predictions of the present relativistic model, in deviation to PPT theory, are shown to be observable using ultrashort laser pulses of relativistic intensities.

DOI: 10.1103/PhysRevA.110.023103

I. INTRODUCTION

The experimental investigation of relativistic strong-field ionization was initiated with the pioneering experiment of Moore *et al.* [1] more than 20 years ago at a laser intensity of 3×10^{18} W/cm^2, demonstrating ionized electron ponderomotive acceleration. Later, in more detailed atomic physics experiments, the observation of signatures of the atomic bound dynamics in photoelectron momentum distributions was investigated in relativistic laser fields [2–9]. Presently, ultrastrong laser fields up to an intensity of 10^{23} W/cm^2 are achievable [10], which provides a good perspective for extending ionization explorations in the relativistic regime.

The state-of-the-art analytical theory of strong-field ionization, the quasiclassical Perelomov-Popov-Terent'ev (PPT) theory [11–16], has been generalized into the relativistic regime [17–20]. The feasibility of observing relativistic features of the ionization yield was recently discussed in Refs. [21,22]. Comparable results are provided by the strong-field approximation (SFA) [23–25], with its relativistic version [26,27]. The PPT theory uses the quasiclassical wave function for the description of the tunneling part of the electron wave packet which is matched to the undisturbed exact bound state. The deficiency of the PPT theory is that the distortion of the bound state in the laser field during the ionization process is not taken into account. This is not essential during tunneling ionization, and the PPT theory well approximates the experimental ionization yield and has been applied for the calibration of ultrahigh laser intensities [28–31]. However, it becomes crucial in the over-the-barrier ionization (OTBI) regime, and from nonrelativistic numerical results it is known that PPT theory significantly overestimates the ionization yield in the latter case [32–36]. The weak-field adiabatic asymptotic theory for the nonrelativistic regime [37–40], treating the Stark shift via perturbation theory, does not fully solve the problem. Why does the PPT theory, seemingly based on the undisturbed bound-state picture, work quite well for strong fields in the tunneling regime? According to Ref. [36], the reason is that the atomic polarization and the Stark shift compensate each other in the tunneling-ionization regime, which, however, fails for OTBI, resulting in the suppression of the ionization yield. We will advocate here that this picture needs to be corrected. We will underline two different contributions of the atomic polarization effect: the shift of the bound state toward the tunnel exit and the bound-state distortion. The first effect, increasing the ionization rate, is implicitly included in PPT theory via the field-dependent matching of the undisturbed bound wave function in the continuum. This is the reason for the good performance of the PPT theory in the tunneling regime. For OTBI, both the bound-state distortion and the Stark shift decrease the rate, causing a substantial discrepancy from PPT theory.

Numerical investigation of the relativistic ionization dynamics, with highly charged ions (HCIs) and ultrastrong laser fields, was carried out in Refs. [28,29,41–52]. In particular, the total ionization yield via a three-dimensional (3D) solution of the Klein-Gordon equation for hydrogenlike HCIs was calculated [52]. The surprising result is that the OTBI yield underestimates by an order of magnitude the prediction of the relativistic PPT theory, with the discrepancy increasing in the deep relativistic regime.

In this paper, a theory of strong-field ionization in the relativistic regime is put forward which incorporates the important effects of the polarization of the atomic bound state and the

*Contact author: klaiber@mpi-hd.mpg.de
†Contact author: k.hatsagortsyan@mpi-hd.mpg.de

Published by the American Physical Society under the terms of the Creative Commons Attribution 4.0 International license. Further distribution of this work must maintain attribution to the author(s) and the published article's title, journal citation, and DOI. Open access publication funded by Max Planck Society.

Stark shift of the bound-state energy in an ultrastrong laser field. We describe the ionization as an adiabatic quantum jump from the bound state in the continuum at a specific transition time. In contrast to the common PPT theory, we account for the bound-state distortion in the laser field using generalized eikonal (GEA) theory [53–55]. The latter improvement is crucial to reproduce the ionization rates from the deep-tunneling up to the OTBI regime, in particular, to explain the order-of-magnitude discrepancies of the numerical result in Ref. [52] for the relativistic ionization with respect to PPT theory. In light of the present theory, the recent experimental results from Ref. [56] are analyzed, and the deviation from PPT theory is explained. We discuss the conditions for an experimental confirmation of the predictions of the present relativistic model versus PPT theory.

The structure of this paper is as follows. In Sec. II the general method of calculation based on the adiabatic transition theory is introduced. In Sec. III the theory for the nonrelativistic regime is developed. For pedagogical reasons, we begin the discussion with the theory for the case of a one-dimensional (1D) short-range atomic potential and further apply the same scheme for a realistic 3D case with a Coulomb potential. The theory is extended into the relativistic regime in Sec. IV, first based on the Klein-Gordon equation and then based on the Dirac equation. The possibility of observing the predictions of our theory is discussed in Sec. V, and the conclusion is given in Sec. VI.

II. ADIABATIC TRANSITION THEORY

Our approach for calculating strong-field ionization probabilities is based on the use of the modified continuum and the bound states. The wave function of the electron is given by the exact time-evolution operator (TEO) $U(t,t')$ of the system:

$$|\psi(t)\rangle = U(t,t^a)|\psi(t^a)\rangle, \tag{1}$$

with the initial condition $|\psi(t^a)\rangle = |\psi_0^a(t^a)\rangle$, where ψ_0^a is the unperturbed atomic bound state at the turn on t^a of the laser field. The ionization amplitude $m_{\mathbf{p}}$ is derived by a projection of ψ on the exact continuum state $\psi_{\mathbf{p}}^f$ with asymptotic momentum $\mathbf{p}$ at the asymptotic time t^f:

$$m_{\mathbf{p}} = \langle\psi_{\mathbf{p}}^f(t^f)|U(t^f,t^a)|\psi(t^a)\rangle, \tag{2}$$

which determines the differential ionization probability:

$$dw/d^3\mathbf{p} = |m_{\mathbf{p}}|^2. \tag{3}$$

We approximate the exact TEO following the Keldysh approach [23], assuming that in the beginning of the ionization process the atomic potential dominates the dynamics, whereas in the end the laser field dominates:

$$U(t^f,t^a) = U^f(t^f,t^*)U^a(t^*,t^a), \tag{4}$$

where U^f is the TEO with a perturbative treatment of the atomic potential V and U^a is the TEO with a perturbative treatment of the laser field. The time t^* is the instant when the transition between the two approximations of the exact TEO takes place. In accordance with the adiabatic transition theory [57–60], the transition time is determined by the condition of the quasienergy equality of the two adiabatically evolved states. The quasienergy of a state is defined as $\varepsilon = -\partial_t S$, with the action S: $\psi = \exp(iS)$. Thus, the transition time from the atomic state modified in the laser field [$\psi^a = \exp(iS^a)$] to the continuum state in the laser field, modified by the Coulomb potential of the atomic core [$\psi^f = \exp(iS^f)$], is found via

$$\partial_t S^a(t^*) = \partial_t S^{f*}(t^*). \tag{5}$$

The adiabatic approximation is valid when the typical timescale of the perturbation exceeds that of the state. For strong-field ionization this implies that the laser period exceeds the atomic evolution time: $\omega \ll I_p$, with ω being the laser frequency and I_p being the atomic ionization potential. The ionization amplitude then takes the simple form of an overlap integral:

$$m_{\mathbf{p}} = \langle\psi_{\mathbf{p}}^f(t^*)|\psi^a(t^*)\rangle. \tag{6}$$

Note, however, that the transition time t^* in Eq. (5) is coordinate dependent, and the overlap integral in Eq. (6) is an integral over possible quantum paths, where each position defines its own switching time t^*.

To derive the modified continuum and bound-state wave functions, we employ GEA theory describing the eikonal S perturbatively. For the continuum wave function the atomic potential is a perturbation in describing the phase, and for the bound state it is a perturbation in the interaction with the laser field.

III. NONRELATIVISTIC REGIME

For pedagogical reasons, we first develop our approach in the case of a 1D short-range atomic potential and further apply the same scheme for a realistic 3D case with a Coulomb potential.

A. One-dimensional model with zero-range potential

We start with the ionization process of an electron bound in a 1D zero-range potential (ZRP),

$$V(x) = -\kappa\delta(x), \tag{7}$$

driven by a constant electric field $E(t) = -E_0$. The electron dynamics is described via the time-dependent Schrödinger equation (TDSE) for the wave function ψ

$$i\partial_t\psi = \left[-\frac{\partial_{xx}}{2} - xE_0 + V(x)\right]\psi. \tag{8}$$

As mentioned above following Eq. (4), U^f is the TEO with a perturbative effect of the atomic potential V and U^a is the TEO, where the electric potential $-xE_0$ is a perturbation.

1. Zeroth-order approximation

In a first step let us use the zeroth-order approximation for the two TEOs:

$$U(t^f,t^a) = U_0^f(t^f,t^*)U_0^a(t^*,t^a), \tag{9}$$

with $U_0^f(t^f,t^*)$ being the Volkov TEO and $U_0^a(t^*,t^a)$ being the atomic TEO. The ionization amplitude in this case takes the simple form of the overlap integral of the wave functions of the Volkov state and the atomic bound state at the switching time t^*. We approximate the laser field by a constant field and use the Volkov wave function in a constant field,

$$\psi_0^f = \frac{1}{\sqrt{2\pi}} \exp\left(iE_0 t x - \frac{iE_0^2 t^3}{6}\right) \tag{10}$$

(vanishing canonical momentum is assumed, $p = 0$, without loss of generality in the case of a static field). The bound state of the atomic potential in the ZRP is

$$\psi_0^a = \sqrt{\kappa} \exp\left(-\kappa|x| + \frac{i\kappa^2 t}{2}\right). \tag{11}$$

Thus, we have the zeroth-order amplitude for ionization:

$$m_0 = \langle \psi_0^f(t^*) | \psi_0^a(t^*) \rangle. \tag{12}$$

The switching time is defined using Eq. (5):

$$\frac{(E_0 t^*)^2}{2} - xE_0 = -I_p, \tag{13}$$

with $I_p = \kappa^2/2$ being the ionization potential. Equation (13) has two solutions:

$$t^* = t_\pm^* \equiv \pm i \frac{\sqrt{2(I_p - xE_0)}}{E_0}. \tag{14}$$

The complexity of the solutions for $x < x_e = I_p/E_0$ indicates the negative kinetic energy at tunneling ionization. Note that only the solution with a positive imaginary part is physical. Mathematically, a physical saddle point is defined by the condition $i\ddot{S}^f(t^*) < i\ddot{S}^a(t^*)$.

For $x > x_e$ there are two real solutions, $t^* = \pm\sqrt{2(xE_0 - I_p)}/E_0$. Since here the electric potential energy xE_0 is initially larger than I_p, i.e., the laser field is not the perturbation anymore, the TEO is approximated by

$$U(t^f, t^a) = U^f(t^f, t_+^*) U^a(t_+^*, t_-^*) U^f(t_-^*, t^a). \tag{15}$$

The dynamics which starts from the tail of the bound wave function out of the barrier is governed initially by the laser field, intermediately by the atom, and finally by the field again. The contribution from these initial coordinates is negligible in a static field with large turn-on and -off times t^a and t^f; consequently, outside of the tunneling barrier no ionization is induced. In physical terms, the electron is free and cannot absorb energy from the laser field in this situation.

The exact numerical calculation of the amplitude m_0 in Eq. (12) is presented in Fig. 1(b). For the analytical estimation we note that the integrand in Eq. (12) has a maximum at $x = 0$ [see Fig. 1(a)], which allows us to expand it for small x, leading to

$$\begin{aligned} m_0 &\approx \int_0 dx \sqrt{\frac{\kappa}{2\pi}} \exp\left(-\frac{E_a}{3E_0} - \frac{E_0\kappa^2 x^2}{2E_a}\right) \\ &= \frac{1}{2}\sqrt{\frac{E_a}{\kappa E_0}} e^{-\frac{E_a}{3E_0}}, \end{aligned} \tag{16}$$

with $E_a = \kappa^3$ being the nonrelativistic atomic field. In the analytical estimation, we neglected the integration region $x < 0$, as it gives a small correction $\sim E_0/E_a$ to the leading term of Eq. (16); see the comparison with the exact numerical integration in Fig. 1(b). As a benchmark, we compare the amplitude

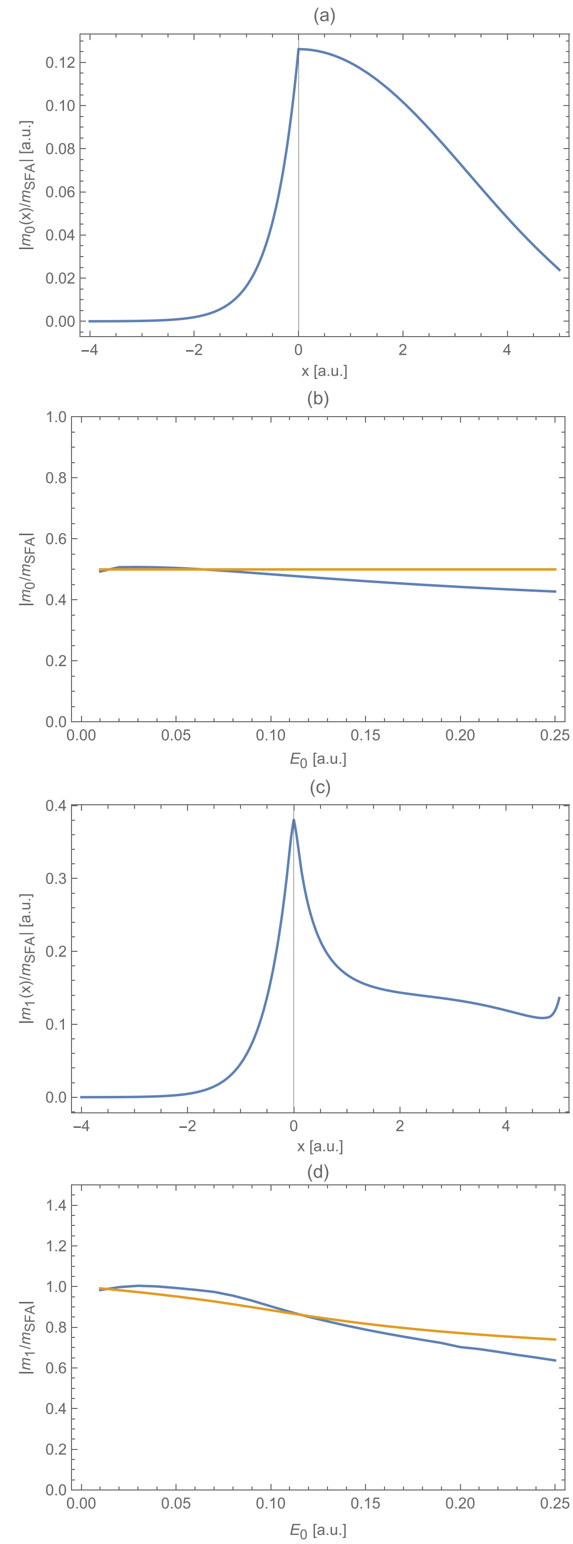

FIG. 1. (a) The integrand of the overlap integral in the zeroth-order description at $E_0 = 0.1$ a.u. (b) Numerically calculated ionization amplitude in the zeroth-order description compared with the first-order SFA result m_0/m_{SFA} (blue) and the analytical estimation using Eq. (16) (orange). (c) The integrand of the overlap integral of Eq. (12) in the first-order description at $E_0 = 0.1$ a.u. (d) The numerically calculated ionization amplitude using the first-order description (25) (blue) and using the exact ionization rate (29) (orange) with respect to that in the first-order SFA.

with that of the first-order SFA for the ZRP. In the zeroth-order approximation we have the relation $m_0/m_{\rm SFA} = 1/2$. This result is also confirmed by the numerical calculation of the overlap integral [see Fig. 1(b)].

2. First-order approximation

We improve the description by taking into account in the first-order approximation the effect of the atomic potential for the continuum motion in the laser field and the effect of the laser field for the bound dynamics. For the description of the continuum motion in the first-order approximation, we replace the Volkov wave function by the GEA wave function in a short-range potential. In this case, the TDSE is rewritten with the ansatz $\psi^f = \exp(iS^f)$ in the following form:

$$-\partial_t S^f = (\partial_x S^f)^2/2 - i\partial_{xx}S^f/2 - xE_0 + V(x). \tag{17}$$

The latter is solved perturbatively with respect to the atomic potential $V(x)$: $S^f = S_0^f + S_1^f$, where the zeroth-order solution coincides with the Volkov phase $S_0^f = E_0 t x - E_0^2 t^3/6$ and the first-order one can be represented in the integral form [55],

$$S_1^f(x,t) = -\frac{\kappa}{2\pi}\int_t ds\sqrt{\frac{2\pi i}{(s-t)}}\exp\left[\frac{(x+\alpha(s)-\alpha(t))^2}{2i(s-t)}\right], \tag{18}$$

with $\alpha(t) = E_0 t^2/2$. Thus, the modified continuum state reads

$$\psi_1^f(x,t) = \psi_0^f(x,t)\exp\left[iS_1^f(x,t)\right]. \tag{19}$$

We can also calculate the second-order correction to the continuum state:

$$S_2^f(x,t) \approx \int_t ds\,\partial_x S_1^f(x,s)^2/2. \tag{20}$$

However, its contribution to the ionization amplitude appears to be negligible and will be further neglected, using $\psi^f(x,t) = \psi_1^f(x,t)$ as the modified continuum state.

In the same way, we consider in the first-order approximation the effect of the laser field for the bound-state dynamics. Using the ansatz $\psi^a = \exp(iS^a)$ for the bound-state wave function, we obtain from the TDSE

$$-\partial_t S^a = (\partial_x S^a)^2/2 - i\partial_{xx}S^a/2 + V - xE_0, \tag{21}$$

which is solved perturbatively with respect to the laser disturbance xE_0: $S^a = S_0^a + S_1^a + S_2^a$. The zeroth-order solution is the bound state $\psi_0^a = \exp(iS_0^a)$ in the ZRP, $S_0^a = i\kappa\sqrt{x^2} + \kappa^2/2t - i\ln(\sqrt{\kappa})$, and the first- and second-order corrections are calculated analytically, assuming that the electric field is turned off adiabatically for infinite positive and negative times:

$$S_1^a(x) = -i\frac{\kappa x(1+|x|\kappa)E_0}{2E_a}, \tag{22}$$

$$S_2^a(x,t) = -\frac{iE_0^2x^2\kappa^2(3+\kappa|x|)}{6E_a^2} - \varepsilon_s t, \tag{23}$$

with the Stark shift $\varepsilon_s = -5/8\kappa^2E_0^2/E_a^2$ of the bound-state energy. All other terms besides the Stark shift describe the polarization of the atomic bound state before the tunnel ionization. Whereas the Stark shift is quadratic in the field, the polarization also has linear terms. Thus, the modified bound state reads

$$\begin{aligned}\psi^a(x,t) &= c_2^a\psi_0^a(x,t)\exp\left[iS_1^a(x) + iS_2^a(x,t)\right]\\ &\approx c_2^a\psi_0^a(x,t)\left\{1 + iS_1^a(x) - \left[S_1^a(x)\right]^2/2 + iS_2^a(x,t)\right\}\\ &= \psi_0^a(x,t)\left\{1 + \frac{E_0\kappa x(1+|x|\kappa)}{2E_a} - i\varepsilon_s t\right.\\ &\quad\left. + \frac{E_0^2\{-30 + x^2\kappa^2[15 + |x|\kappa(10+3x\kappa)]\}}{24E_a^2}\right\},\end{aligned} \tag{24}$$

where $c_2^a = 1 - 5E_0^2/4E_a^2$ is the normalization constant. Here, the correction is expanded into the preexponential, which is equivalent to the perturbation theory with respect to the xE_0 potential.

We calculate the ionization amplitude including the leading-order correction:

$$m_1 = \int dx\,\psi^f(x,t^*)^*\psi^a(x,t^*). \tag{25}$$

The overlap integral above is calculated numerically up to the tunnel-exit coordinate $x_e = I_p/E_0$. This choice of the upper limit of the coordinate integration of the overlap integral with an approximate wave function, Eq. (24), is justified in the next section, where it is compared with the exact case. Further, Fig. 1(d) confirms that the ionization probability with modified wave functions for the case of the ZRP is in accordance with the first-order SFA in weak fields.

3. One-dimensional exact case

To judge the accuracy of the applied approximations in the previous sections, we compare the ionization amplitude using the first-order description in Eq. (25) with the exact solution. The Schrödinger equation (8) in the 1D case for electron ionization from a bound state in a δ potential has an exact solution, expressed via Airy functions. We look for the energy eigenstate in the potential $-\kappa\delta(x) - xE_0$:

$$\psi(x,t) = \psi(x)\exp(-i\varepsilon t), \tag{26}$$

imposing the standard boundary conditions to $\psi(x)$, corresponding to the ionization problem: the current density is positive at $x\to\infty$, describing an outgoing wave, and the probability is vanishing at $x\to-\infty$. This yields the solution for the energy ε,

$$\begin{aligned}\psi_+(x) &= c_+\left(\mathrm{Bi}\left[-\frac{2^{1/3}(\varepsilon+E_0x)}{E_0^{2/3}}\right]\right.\\ &\quad\left.+ i\mathrm{Ai}\left[-\frac{2^{1/3}(\varepsilon+E_0x)}{E_0^{2/3}}\right]\right), \quad x>0,\\ \psi_-(x) &= c_-\mathrm{Ai}\left[-\frac{2^{1/3}(\varepsilon+E_0x)}{E_0^{2/3}}\right], \quad x<0.\end{aligned} \tag{27}$$

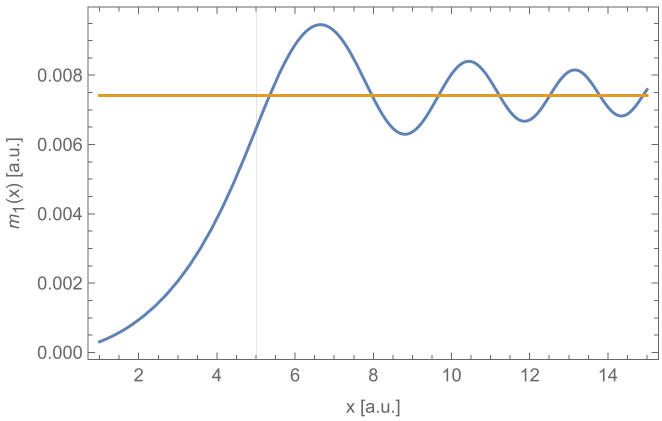

FIG. 2. The overlap integral of Eq. (25) for $E_0 = 0.1$ a.u. with the exact atomic wave function of Eq. (27) calculated up to the coordinate x: $m_1(x) = \int_{-\infty}^{x} dx\, \psi^f(x,t^*)^* \psi^a(x,t^*)$. The vertical grid line is the tunnel exit $x_e = I_p/E_0$. At $x = x_e$, the overlap integral is stabilized to a certain value.

Further, we impose the continuity conditions for the wave function and for its derivative:

$$\psi_+(0) = \psi_-(0),$$
$$\psi_+'(0) - \psi_-'(0) = -2\kappa\psi_+(0), \tag{28}$$

which are solved numerically, providing complex eigenenergy ε and the ratio c_+/c_-.

The ionization rate is described by the imaginary part of the complex eigenenergy,

$$\Gamma = -2\mathrm{Im}\{\varepsilon\}. \tag{29}$$

The result of the comparison of the exact ionization rate with that from the first-order description in Eq. (25) is shown in Fig. 1(d) for different field strengths, where both are given with respect to the SFA value $\Gamma_{\mathrm{SFA}} = \kappa^2 \exp[-(2/3)(\kappa^3/E_0)]$. Figure 1(d) shows that the first-order description with our model provides a good approximation of the exact ionization rate.

The value of the overlap integral in Eq. (25) with the exact atomic wave function in Eq. (27), depending on the upper bound of the coordinate, is shown in Fig. 2. It indicates that the integral value is stabilized at the tunnel exit in the exact case. In the region $x > x_e$, the integral oscillates, and the net contribution from this region is vanishing. The latter justifies the restriction of the integration region of the overlap integral up to $x = x_e$ in the case of the approximate modified atomic wave function.

4. *Time-dependent laser field: Quasistatic approximation*

In the quasistatic approximation, the results obtained with a constant laser field E_0 are still valid for the case of a time-dependent laser field $E(t)$ using the replacement $E_0 \to E(t)$. Let us estimate the validity condition of this approximation by inserting the quasistatic solution into the exact differential equation in the 1D case, Eq. (17). Using the analytical expression from Ref. [61] for the matching time $t^* = \arcsin(i\gamma)/\omega - ix_s/\kappa$ and the estimate for the typical value of the coordinate for the tunneling $x_s \sim \sqrt{\kappa/E_s}$, with $E_s \equiv E(t_s) = E_0\sqrt{1+\gamma^2}$ and the Keldysh parameter [23] $\gamma = \kappa\omega/E_0$, the error of the approximate solution to Eq. (17) scales as $(E_0/E_a)\gamma \sim \omega/I_p$, which gives the condition of the applicability of the quasistatic approximation.

B. Three-dimensional case with Coulomb potential

The method outlined within a 1D simple model in the previous section is applied here for a realistic 3D case with a Coulomb potential. The Schrödinger equation for the eikonal S reads, in this case,

$$-\partial_t S = (\nabla S)^2/2 - i\Delta S/2 + V(r) + \mathbf{r}\cdot\mathbf{E}(t). \tag{30}$$

The description of the continuum motion is modified, treating the atomic potential $V(r) = -Z/r$, with Z being the charge of the atomic core, by the perturbation theory in Eq. (30):

$$S^f = S_0^f + S_1^f, \tag{31}$$

where the unperturbed eikonal [at $V = 0$] corresponds to the nonrelativistic Volkov wave function $\psi_{\mathbf{p},0}^f$ [62],

$$S_0^f = [\mathbf{p} + \mathbf{A}(t)]\cdot\mathbf{r} + \int_t dt'[\mathbf{p} + \mathbf{A}(t)]^2/2, \tag{32}$$

with $\mathbf{A}(t) = -\int \mathbf{E}(t)dt$, and the perturbed eikonal S_1^f fulfills the equation

$$-\partial_t S_1^f - [\mathbf{p} + \mathbf{A}(t)]\cdot\nabla S_1^f + i\Delta S_1^f/2 = V(r). \tag{33}$$

The solution of Eq. (33) is known from the GEA theory [55]:

$$S_1^f(\mathbf{r},t) = -Z\int_t ds \frac{\mathrm{erf}\Big[\sqrt{\frac{[\mathbf{r}+\mathbf{p}(s-t)+\boldsymbol{\alpha}(s)-\boldsymbol{\alpha}(t)]^2}{-2i(s-t)}}\Big]}{\sqrt{[\mathbf{r}+\mathbf{p}(s-t)+\boldsymbol{\alpha}(s)-\boldsymbol{\alpha}(t)]^2}}, \tag{34}$$

where $\boldsymbol{\alpha}(t) = \int dt\mathbf{A}(t)$ is the displacement in the laser field and S_1^f describes the modification of the tunneling barrier due to the Coulomb field, enhancing the ionization probability [14].

In a similar manner, the description of the bound-state dynamics is modified, treating the interaction with the laser field as a perturbation in the eikonal in Eq. (30):

$$S^a = S_0^a + S_1^a, \tag{35}$$

where the unperturbed eikonal corresponds to the free atomic wave function [63],

$$S_0^a(\mathbf{r},t) = i\kappa r - i(Z/\kappa - 1)\ln(\kappa r)$$
$$- i\ln(\sqrt{\kappa^3/\pi}) + I_p t + c_0^a, \tag{36}$$

with $\kappa = \sqrt{2I_p}$ being the atomic velocity and c_0^a being the normalization constant. The perturbed eikonal S_1^a describes the polarization of the atomic state in the laser field and fulfills

$$-\partial_t S_1^a - \nabla S_0^a\cdot\nabla S_1^a + i\Delta S_1^a/2 = \mathbf{r}\cdot\mathbf{E}(t). \tag{37}$$

First, we consider the quasistatic case $\mathbf{E}(t) = -\hat{\mathbf{x}}E_0 =$ const (with $p_x = 0$ without loss of generality). With parabolic coordinates $u = \sqrt{r+x}$ and $v = \sqrt{r-x}$, the solution close to the origin is

$$-E_0u^4 - if_u''(u) + 2i\kappa u f_u'(u) - \frac{if_u'(u)}{u}$$
$$+ E_0v^4 - if_v''(v) + 2i\kappa v f_v'(v) - \frac{if_v'(v)}{v} = 0, \tag{38}$$

with $S^a = f_u + f_v$. The 2D differential equation is then separated,

$$-E_0u^4 - if_u''(u) + 2i\kappa u f_u'(u) - \frac{if_u'(u)}{u} = -2E_0/\kappa^2,$$
$$+E_0v^4 - if_v''(v) + 2i\kappa v f_v'(v) - \frac{if_v'(v)}{v} = 2E_0/\kappa^2. \quad (39)$$

The first-order correction reads

$$S_1^a = -\frac{iE_0u^2(4+u^2\kappa)}{8\kappa^2} + \frac{iE_0v^2(4+v^2\kappa)}{8\kappa^2}. \quad (40)$$

In the same manner, the second-order solution is derived as

$$S_2^a = -\frac{iE_0^2(u^4\kappa(21+2u^2\kappa))}{96\kappa^5} - \frac{iE_0^2(v^4\kappa(21+2v^2\kappa))}{96\kappa^5} - \varepsilon_s t \quad (41)$$

with the Stark energy shift $\varepsilon_s = -9\kappa^2E_0^2/4E_a^2$ (cf. [63]). Thus, we have the following modified bound state:

$$\psi^a(\mathbf{r},t) = c_2^a\psi_0^a(\mathbf{r},t)\exp\left(iS_1^a + iS_2^a\right) \quad (42)$$

$$\approx c_2^a\psi_0^a\left[1 + iS_1^a - \left(S_1^a\right)^2/2 + iS_2^a\right]$$
$$\approx \psi_0^a(\mathbf{r},t)\left\{1 + \kappa x(2+r\kappa)\frac{E_0}{2E_a} - i\varepsilon_s t + \frac{-372+\kappa^2[45x^2+2r^3\kappa+30rx^2\kappa+3r^2(7+2x^2\kappa^2)]}{48} \times\left(\frac{E_0}{E_a}\right)^2\right\}, \quad (43)$$

with the normalization constant $c_2^a = 1 - 31E_0^2/4E_a^2$. We expanded the exponent as $S_{1,2}^a \ll 1$ at $r \sim 1/\kappa$. With the replacement $E_0 \to E(t)$, the solutions above for $S_{1,2}^a$ are also valid in time-dependent fields at $(E_0/E_a)\gamma^2/\sqrt{1+\gamma^2} \ll 1$, with the atomic field $E_a \equiv \kappa^3$, which is equivalent to $\omega/I_p \ll 1$ at a large Keldysh parameter $\gamma = \kappa\omega/E_0$ [23].

The ionization amplitude is calculated numerically using Eq. (6) with the modified wave functions ψ^f and ψ^a. The integration over the coordinate in Eq. (6) is extended up to the tunnel exit $x_e = I_p/E_0$, as the tail of the wave function out of the barrier cannot contribute to ionization. The calculated ionization rate w, highlighting different contributions, is illustrated in Fig. 3. It is remarkable that it accurately reproduces the Tong-Lin fitting factor [34] of the ionization yield via numerical TDSE solutions with respect to PPT theory:

$$T_{\rm nr} \equiv \left(\frac{w}{w_{\rm PPT}}\right)_{\rm nonrel} = \exp\left[-\left(\frac{Z^2}{\kappa^2}\right)\left(\frac{12E_0}{E_a}\right)\right], \quad (44)$$

with $w_{\rm PPT}$ being the PPT rate [16]. We analytically estimate the Tong-Lin factor with our model at $f \equiv E_0/E_a \ll 1$ in Appendix A.

We highlight the following contributions in Fig. 3: the Stark shift described via the eikonal term $\varepsilon^s t$, the polarization effect as a shift of the bound state toward the tunnel exit (via S_1^a and $S_2^a + \varepsilon^s t$), and the polarization effect of the bound-state distortion (via the factor c_2^a). The shift of the bound state increases the ionization rate (by a factor of ∼4) up to the PPT value for weak fields. This is because the PPT rate implicitly includes this polarization effect via the field

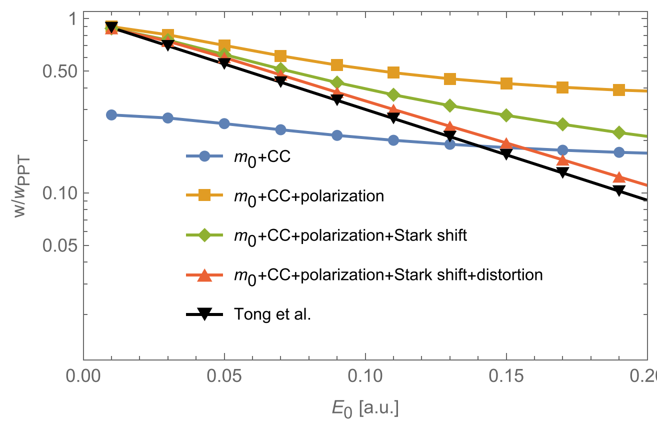

FIG. 3. The ratio of the ionization rate w to that of PPT-theory $w_{\rm PPT}$ for hydrogen ($\kappa = 1$): blue circles, our model with only Coulomb corrections (CCs) via S_1^f; orange squares, our model with CCs and the atomic polarization (via S_1^f, S_1^a, and $S_2^a + \varepsilon^s t$); green diamonds, our model with CCs, the atomic polarization, and the Stark shift; red triangles, our model with all corrections, including the bound-state distortion; black inverted triangles, the Tong-Lin factor [34].

dependence of the matching coordinate $x_s = \sqrt{\kappa/E_0}$ of the undisturbed bound wave function in the continuum. This is the reason for the good performance of the PPT theory in the tunneling regime. In strong fields, the bound-state distortion and the Stark shift decrease the rate away from the PPT result with the respective scalings $\sim -15E_0^2/E_a^2$ and $\sim -5E_0/E_a$, according to our model. Note that the Stark shift of a hydrogen atom in a static electric field in the nonrelativistic regime was previously addressed in many publications that proposed, in particular, different techniques for the resummation of the divergent perturbation series (see, e.g., [64–67] and references therein). In contrast, our aim here is to put forward a simple scheme for a perturbative treatment, with a benchmark of the Tong-Lin factor, and apply this to the relativistic regime.

IV. RELATIVISTIC REGIME

We apply our theory to the relativistic regime described by the Klein-Gordon equation as well as by Dirac equations.

A. Klein-Gordon equation

In the case of the Klein-Gordon equation we look for the solution using the ansatz $\psi = \exp(i\mathcal{S})$, where the eikonal $\mathcal{S}$ fulfills the equation [54]

$$-i\partial^2\mathcal{S}(x) + [\partial\mathcal{S}(x) + A(\eta)/c + V(x)/c]^2 = c^2, \quad (45)$$

where the four-coordinate $x_\mu = (ct, \mathbf{r})$, $\partial \equiv \partial/\partial x_\mu$, the laser four-vector potential $A(\eta) = (\mathbf{r}\cdot\mathbf{E}(\eta), -\hat{\mathbf{k}}(\mathbf{r}\cdot\mathbf{E}(\eta)))$ in the Göppert-Mayer gauge, $\hat{\mathbf{k}} = \mathbf{k}/|\mathbf{k}|$, $\mathbf{k}$ is the laser wave vector, and the atomic four-potential $V(x) = (V(r), 0, 0, 0)$. The gauge invariance of the theory is discussed in Appendix D. The eikonal is derived using perturbation theory,

$$\mathcal{S} = \mathcal{S}_0 + \mathcal{S}_1, \quad (46)$$

either with respect to V for $\mathcal{S}^f$ or with respect to $A(\eta)$ for $\mathcal{S}^a$.

1. Modified continuum wave function

The unperturbed eikonal of the relativistic continuum state $\mathcal{S}_0^f$ is represented by the phase of the relativistic Volkov wave function [68]:

$$\mathcal{S}_0^f(x,y,z,t)=[p_x+A(\eta)]x+p_y y-c\Lambda z-\int_\eta ds\tilde{\varepsilon}(s). \tag{47}$$

Here, the laser wave propagates along the z axis and is linearly polarized along the x axis, $\eta=t-z/c$, $\Lambda\equiv\varepsilon/c^2-p_z/c$ is the motion integral in a plane wave field, $\varepsilon=\sqrt{c^4+c^2p^2}$ is the electron energy, and $\tilde{\varepsilon}(s)=\varepsilon+[p_xA(\eta)+A(\eta)^2/2]/\Lambda$ is the energy in the laser field. The GEA correction to the eikonal of the continuum state $\mathcal{S}_1^f$ fulfills the equation

$$-i\partial^2\mathcal{S}_1^f(x)+2\big[\partial\mathcal{S}_0^f(x)+A(\eta)/c\big]\big[\partial\mathcal{S}_1^f(x)+V(x)/c\big]=0. \tag{48}$$

After coordinate transformation to $(\eta,\mathbf{r})$, Eq. (48) is solved via a Fourier transformation. In the case of a quasistatic field, using the zeroth-order solution in the velocity gauge $\mathcal{S}_0^f=-c\Lambda z-\varepsilon\eta-E_0^2\eta^3/(6\Lambda)$ ($p_{x,y}=0$ in the constant field), the equation for the Fourier component is

$$\sqrt{\frac{2}{\pi}}Z\Big[p_zE_0^2\eta^2+\frac{\varepsilon}{c}\big(2c^2+E_0^2\eta^2\big)\Big]+cq^2\left\{\big[ic\Lambda q_zE_0^2\eta^2+c^2(q^2+2p_zq_z+2q_xE_0\eta)\big]\tilde{\mathcal{S}}_1^f(\eta,\mathbf{q})+2c(c\Lambda-q_z)\frac{\partial\tilde{\mathcal{S}}_1^f(\eta,\mathbf{q})}{\partial\eta}\right\}=0,$$

which is solved exactly. The solution is simplified at $q_z\ll c$:

$$\tilde{\mathcal{S}}_1^f(\eta,\mathbf{q})\approx-Z\int_\eta ds\exp\left(\frac{i(s-\eta)}{6c^2\Lambda}\big\{c\Lambda q_zE_0^2(s^2+s\eta+\eta^2)+3c^2[q^2+2q_zp_z+q_xE_0(s+\eta)]\big\}\right)\frac{2\varepsilon+c\Lambda E_0^2s^2}{\sqrt{2\pi}c^3\Lambda q^2}. \tag{49}$$

In the coordinate space the eikonal for the relativistic continuum reads

$$\mathcal{S}_1^f(\eta,\mathbf{r})\approx-Z\int_\eta ds\frac{\tilde{\varepsilon}(s)\mathrm{erf}\Big[\sqrt{\Lambda\frac{r(s,\eta)^2}{-2i(s-\eta)}}\Big]}{c^2\Lambda r(s,\eta)}, \tag{50}$$

with the relativistic trajectory $r(s,t)=(\{x+[\alpha(s)-\alpha(\eta)]/\Lambda\}^2+[y+p_y(s-\eta)/\Lambda]^2+\{z+p_z(s-\eta)/\Lambda+[\beta(s)-\beta(\eta)]/(c\Lambda^2)\}^2)^{1/2}$, and $\beta=\int d\eta A^2(\eta)/2$.

2. Modified bound-state wave function

The unperturbed relativistic bound-state wave function is known from the atomic theory [20,63] with

$$\mathcal{S}_0^a=S_0^a-i[(1-I_p/c^2)^2-1]\ln(\kappa r)-i\ln\big(C_0^a\big), \tag{51}$$

where S_0^a is the nonrelativistic term from Eq. (36) and $C_0^a=2^{-1+\epsilon_0^2}/\sqrt{2c\epsilon_0\Gamma(2\epsilon_0^2)}$, with $\epsilon_0\equiv1-I_p/c^2$.

The correction to the bound state fulfills the equation

$$-i\partial^2\mathcal{S}_1^a(x)+2\big[\partial\mathcal{S}_0^a(x)+V(x)/c\big]\big[\partial\mathcal{S}_1^a(x)+A(\eta)/c\big]=0 \tag{52}$$

and a similar equation for $\mathcal{S}_2^a$. The equations for $\mathcal{S}_{1,2}^a$ are solved in a quasiclassical expansion over $\hbar$ [69], where we go to next to leading order in $\hbar$. The main corrections to the bound state come from the atomic polarization and Stark shift due to the laser electric field. Additionally, new terms in the relativistic regime occur due to the laser magnetic field and the electron mass correction. The leading-order correction up to E_0/E_a and $\hbar$ is derived from following equation:

$$\partial_r\mathcal{S}_1^{\mathrm{cor}}=\left(-\frac{E_axz}{cr}-i\frac{E_ax}{\kappa}+i\frac{E_aI_px}{c^2\kappa}+ix\kappa^2\right)\frac{E_0}{E_a}, \tag{53}$$

where $\mathcal{S}_1^{\mathrm{cor}}\equiv\mathcal{S}_1-S_1^a$, S_1^a is the nonrelativistic term from Eq. (40), and $E_a=\sqrt{3}\sigma^3/(1+\sigma^2)c^3$ is the relativistic atomic field [20] with $\sigma=\sqrt{2+\epsilon_0^2-\epsilon_0\sqrt{8+\epsilon_0^2}}/\sqrt{2}$. Therefore, finally, we have

$$\mathcal{S}_1^a=S_1^a+ix\left\{\frac{-E_a(1-I_p/c^2)r+iE_az\kappa/c+r\kappa^3}{2\kappa}+\frac{\kappa^3-E_a[(1-I_p/c^2)^3+Z\kappa/c^2]}{\kappa^2}\right\}\frac{E_0}{E_a}. \tag{54}$$

The higher-order correction is calculated in a similar way:

$$\begin{aligned}\mathcal{S}_2^a = S_2^a + \Bigg\{ & \frac{ir\big[\kappa^6 r^2 - \frac{E_a^2(c^2(-r)+ic\kappa z+rI_p)^2}{c^4}\big]}{24\kappa^3} - \frac{irx^2\big\{3E_a^2\big[\big(\frac{I_p}{c^2}-1\big)^2+\frac{\kappa^2}{c^2}\big]-3\kappa^6\big\}}{24\kappa^3}\\ & - \frac{E_a^2 rz\big[11c^6 + c^4(6\kappa Z - 29I_p) + 27c^2 I_p^2 - 9I_p^3\big]}{24c^7\kappa^3}\\ & - \frac{ir^2\big[-21c^8\kappa^6 - c^6E_a^2\kappa^2 + 3E_a^2(c^2-I_p)^2\big(7c^4 - 10c^2I_p + 5I_p^2\big) + 12c^4E_a^2\kappa Z(c^2-I_p)\big]}{48c^8\kappa^4}\\ & - \frac{i\big[-7c^8\kappa^6x^2 + 7E_a^2x^2(c^2-I_p)^4 + c^2E_a^2\kappa^2\big[c^4(4x^2+y^2) + 2c^2I_p(z^2-3x^2) + I_p^2(3x^2-z^2)\big] + 4c^4E_a^2\kappa x^2 Z(c^2-I_p)\big]}{16c^8\kappa^4}\Bigg\}\\ & \times\left(\frac{E_0}{E_a}\right)^2, \end{aligned} \tag{55}$$

where S_2^a is the nonrelativistic term from Eq. (41).

B. Dirac equation

Our starting point is the quadratic Dirac equation:

$$[(i\partial + A/c + V/c)^2 - c^2 + \Sigma\cdot\mathbf{B}/c + i\boldsymbol{\alpha}\cdot\mathbf{E}/c]\psi = 0. \tag{56}$$

The wave function of the latter is looked for using the ansatz $\psi = u\exp(i\mathcal{S})$, where u is the spinorial part and $\mathcal{S}$ is the eikonal of the Klein-Gordon equation. We look for the solution of u and $\mathcal{S}$ perturbatively with respect to the atomic potential and the laser field for the modified continuum and bound state, respectively.

The unperturbed wave function of the relativistic continuum state of the Dirac equation $u_0^f\exp(i\mathcal{S}_0^f)$ is represented by the relativistic Volkov wave function [68]. The correction $\mathcal{S}_1^f$ to the eikonal of the modified continuum wave function is given by Eq. (50). We neglect u_1^f, which describes the spin flip induced by the atomic potential during the tunneling dynamics and is of the order of $(\kappa/c)^3$ according to Ref. [69].

The unperturbed relativistic bound-state wave function for the Dirac equation is given by [63]

$$\mathcal{S}_0^a = S_0^a - iI_p/c^2\ln(\kappa r) - i\ln\left(C_0^a\right), \tag{57}$$

with $C_0^a = 2^{-1+\epsilon_0}\sqrt{(1+\epsilon_0)/\Gamma(1+2\epsilon_0)}$. We choose the Dirac eikonal for the atomic wave function to be identical to the Klein-Gordon one $\mathcal{S}^a$ and find the spinorial corrections. The first-order spinorial correction in $\hbar$ and E_0/E_a is then a solution of the following equation:

$$\begin{aligned}(4c^2 - I_p)\partial_r u_1^a = {} & 4I_pc\big(1 + 2\varepsilon_M\dot{u}_1^a, 2\varepsilon_M\dot{u}_1^a, 2\varepsilon_M\dot{u}_1^a, 2\varepsilon_M\dot{u}_1^a\big)\\ & - \left(\frac{i(2I_p)^{3/2}(z+3ix)}{r}, \frac{i(2I_p)^{3/2}y}{r}, -\frac{2iI_pcxy}{r^2}, \frac{(2I_p)^{3/2}r(x-iz) + 2cI_p[r^2 + x(x-iz)]}{r^2}\right)\frac{E_0}{E_a},\end{aligned} \tag{58}$$

where $\varepsilon_M = -E_0/(2c)$ and $1/c$ expansion up to second order was applied. The solution of the latter equation reads

$$u_1^a = i\frac{E_0 t}{2c}u_0^a + \frac{E_0}{E_a}\begin{bmatrix} \frac{I_p^{3/2}(-iz+3x)}{\sqrt{2}c^2} \\ \frac{iI_p^{3/2}y}{\sqrt{2}c^2} - \frac{I_pr}{c} \\ -\frac{iI_pxy}{2rc} - \frac{I_pr}{c} + i\frac{I_p^{3/2}y}{\sqrt{2}c^2} \\ -\frac{-I_p(z^2+izx+y^2)}{2rc} \end{bmatrix}. \tag{59}$$

Using the modified atomic and continuum wave functions in the relativistic regime, $\psi^a = C_2^a\{\psi_0^a[1 + i\mathcal{S}_1^a - (\mathcal{S}_1^a)^2/2 + \mathcal{S}_2^a] + \exp(i\mathcal{S}_0^a)(u_1^a + i\mathcal{S}_1^a u_1^a + u_2^a)\}$, the ionization amplitude of Eq. (6) for the Klein-Gordon and Dirac equations is calculated numerically at the most probable momentum $\mathbf{p} = (0, 0, I_p/3c)$ [70]; see Fig. 4, where the ionization yields from different approximations are compared.

We also estimated analytically the relativistic analog of the Tong-Lin factor (the correction factor to the PPT ionization rate):

$$\left(\frac{w}{w_{\rm PPT}}\right)_{\rm rel} \approx \left(\frac{w}{w_{\rm PPT}}\right)_{\rm nr} e^{-\frac{2\kappa^2}{c^2}} \approx \exp\left(-\frac{12Z^2}{\kappa^2}\frac{E_0}{E_a} - \frac{2\kappa^2}{c^2}\right). \tag{60}$$

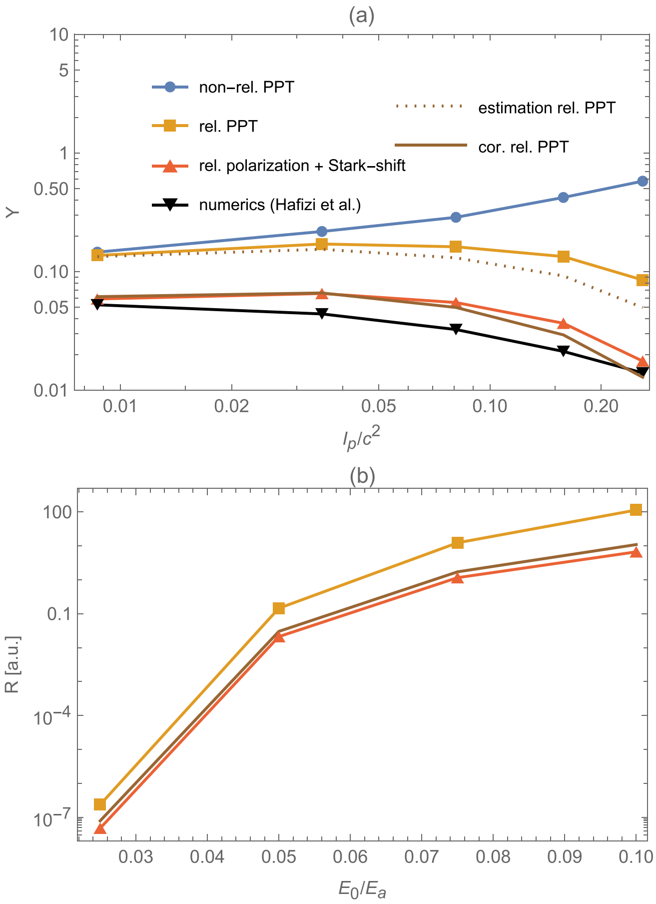

FIG. 4. Analytical estimates for the relativistic ionization: (a) The ionization yield (Y). (b) The ionization rate (R). In both panels symbols are as follows: blue circles, nonrelativistic PPT theory; orange squares, relativistic PPT theory; red triangles, corrected relativistic rates from the present theory; black inverted triangles, corrected relativistic rates from the numerical solution of the Klein-Gordon equation in Ref. [52]; dotted line, the analytical estimate of the PPT rate from Eq. (B1); solid brown line without markers, the analytical estimate of the corrected relativistic PPT rate via the Tong-Lin factor (60).

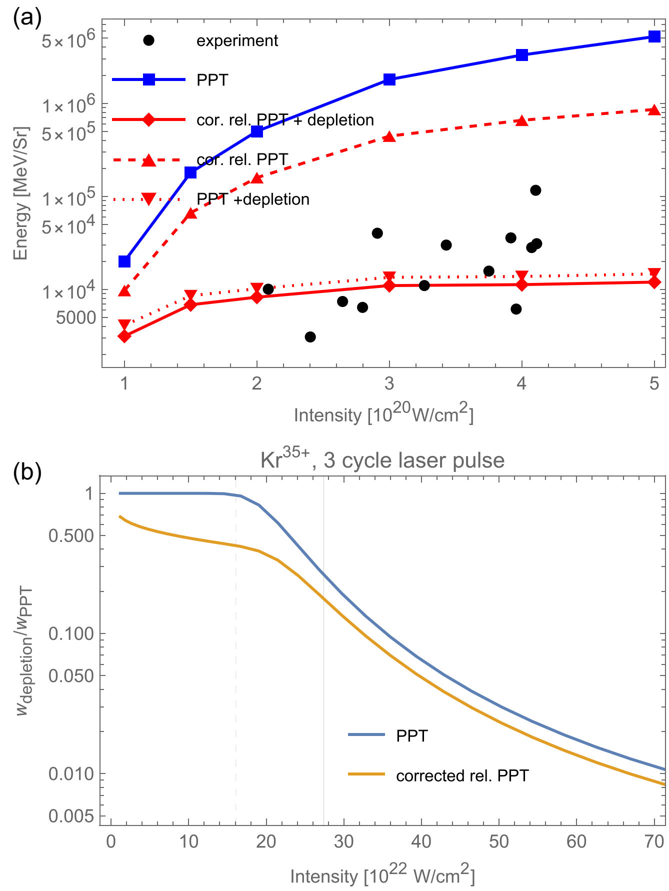

FIG. 5. (a) Integrated electron energy vs laser intensity: the experimental results of Ref. [56] with the 1-mm shield (black circles), the PPT theory from Ref. [56] (blue solid squares), PPT theory with depletion (red dotted line with inverted triangles), the corrected PPT theory with the present model (red dashed line with triangles), and our model including the depletion effect of the ground state (red diamonds). (b) The ratio of the ionization yield for Kr^{35+} with respect to PPT in a three-cycle laser pulse for the PPT yield with depletion (blue line) and our model with depletion (orange line). The grid lines show the OTBI threshold (solid) and the saturation intensity for Kr^{34+} (dashed).

The relation between the relativistic and nonrelativistic ionization rates is given in Appendix B.

In Fig. 4 the relativistic correction factor for the PPT theory given above is tested against the matching method in this paper as well as against the numerical calculation in Ref. [52], demonstrating good performance. According to Fig. 4, our theory provides good agreement for the yield with the results of the numerical solution of the Klein-Gordon equation from Ref. [52], while the standard relativistic PPT theory overestimates it by more than an order of magnitude. The role of the different polarization effects (bound-state shift and distortion) and the Stark shift is similar to that in the nonrelativistic case (Fig. 3). The main characteristic feature of the relativistic yield is the decreasing of the yield at large I_p/c^2. This stems from the relativistic mass shift effect, which decreases the size and the polarization of the atomic bound state at large I_p/c^2. The latter contributes to the deviation of the result with our model from that of the relativistic PPT theory.

V. POSSIBILITIES FOR OBSERVING THE THEORY PREDICTIONS

Recently, an experiment on tunneling ionization from the K shell of neon in the relativistic regime was carried out with a laser intensity exceeding 10^{20} W/cm^2 [56]. The integrated electron energy was measured. The authors also provided Monte Carlo simulations employing the PPT rates and concluded that the PPT theory (as well as the so-called barrier-suppression ionization model [71]) overestimates the ionization yield. However, it appears that the depletion of the atomic state is not taken into account in these simulations. We give an estimation of the experimental results using the theoretical method in this paper and include the depletion effect. Our qualitative estimation consists of multiplying the PPT curve in Fig. 5(a) by the correction factor according to our theory $(w/w_{\rm PPT})_{\rm rel}$. The depletion is accounted for by evaluating the correction factor for the laser

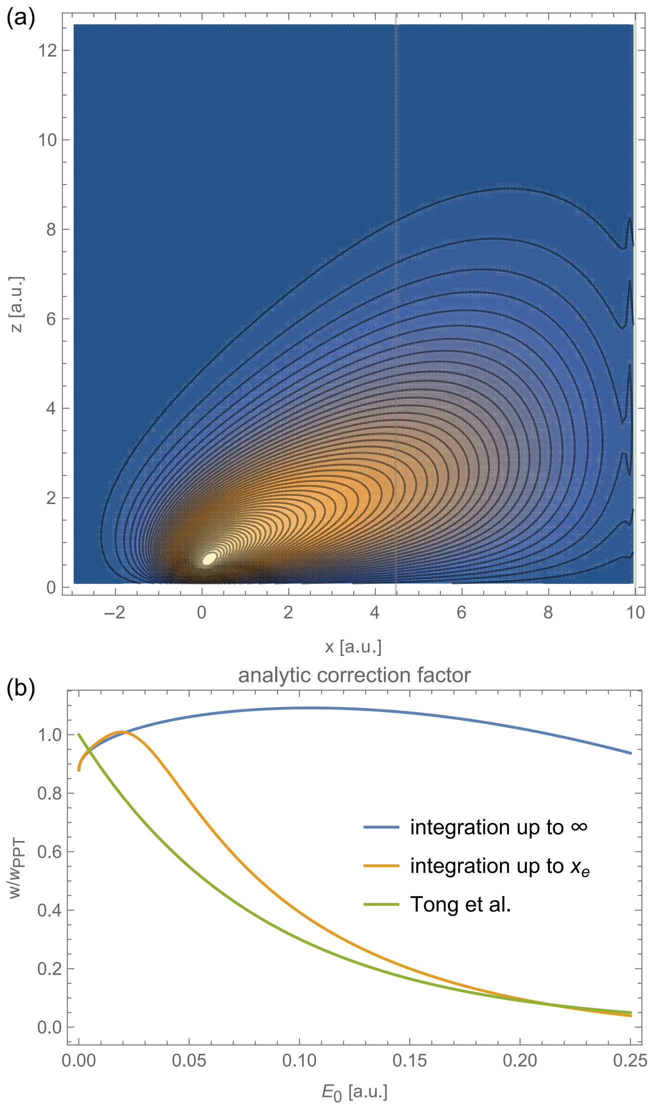

FIG. 6. (a) The m_1 integrand for the Coulomb case at $E_0 = 0.05$ a.u. (b) Analytic estimates of the correction factor via Eqs. (A2) and (A3); the green line shows the Tong-Lin factor [34].

field corresponding to the ionization saturation time t_d, determined from the ionization yield $Y(t)$ via $\ddot{Y}(t_d) = 0$ (see Appendix C). When the depletion of the bound state is included, both the PPT theory and our method fit the experimental result within the experimental error [Fig. 5(a), red solid and red dotted lines], Thus, the experimental result from Ref. [56] cannot distinguish between PPT theory and our method. This is because of the domination of the depletion over a long laser pulse duration in the experiment (25 cycles). With a shorter laser pulse, the deviation of our method from PPT theory is measurable near the OTBI threshold, as the example of krypton HCI ionization in a three-cycle ultraintense laser pulse demonstrates in Fig. 5(b). We see that near the OTBI threshold, accounting for the bound-state distortion in the laser field can result in a decrease in the ionization yield by more than 2 times.

VI. CONCLUSION

We put forward a simple model for relativistic ionization with the important ingredient of accounting for the bound-state polarization and the Stark shift beyond perturbation theory. With this modification to the adiabatic transition model, the deviation of the numerical and experimental results from the PPT theory was explained. In the recent experiment in Ref. [56] the depletion of the bound state was the dominating factor to account for the deviation from PPT theory. The role of depletion can be avoided by using shorter laser pulses, with which the prediction of our model deviating from PPT theory can be confirmed.

ACKNOWLEDGMENT

We thank A. Yandow for providing the experimental data. M.K. acknowledges fruitful discussions with J. S. Briggs.

APPENDIX A: ANALYTICAL ESTIMATE FOR THE MODIFIED IONIZATION AMPLITUDE

We provide an analytical estimate for the modified ionization amplitude m_1. First of all, we approximate the 3D overlap integral via that of the 1D case using the result in Ref. [72]:

$$m_1 = c_{3D} \int dx C(x) \psi_0^f(x, t^*) \psi_0^a(x, t^*) \times \left\{1 + i S_1^a(x, 0) - \left[S_1^a(x, 0)\right]^2 + i S_2^a(x, 0)\right\}, \quad \text{(A1)}$$

with the Coulomb-correction factor of the PPT theory $C(x) = \sqrt{8}(E_a/E_0)(1 - E_0 x/\kappa^2 - E_0^2 x^2/4\kappa^4)$ [69], the dimensional conversion factor $c_{3D} = 1/\sqrt{2\pi\kappa^2}$ [72], and the polarization corrections $S_1^a(x, 0)$ and $S_2^a(x, 0)$ on the x axis in the case of Coulomb potential.

The integrand is shown in Fig. 6(a), justifying the integration along the x axis ($y = z = 0$; note that the volume element z is included in the plot). The integration performed until the tunnel exit x_e yields

$$\frac{m_1^{x_e}}{m_{\rm PPT}} = e^{-\frac{1}{8}/f}\left(-\frac{1}{32\sqrt{2\pi} f^{3/2}} - \frac{271\sqrt{f}}{24\sqrt{2\pi}} - \frac{29}{24\sqrt{2\pi}\sqrt{f}}\right) + \frac{4}{3}\sqrt{\frac{2}{\pi}}\sqrt{f} + \frac{15}{8}, \quad \text{(A2)}$$

while the integration up to $x = \infty$ is

$$\frac{m_1^{\infty}}{m_{\rm PPT}} = \frac{9 f^{3/2}}{2\sqrt{2\pi}} - \frac{53 f^2}{8} - \frac{9 f}{8} + \frac{4}{3}\sqrt{\frac{2}{\pi}}\sqrt{f} + \frac{15}{8}, \quad \text{(A3)}$$

with $f = E_0/E_a$.

From Fig. 6(b) one can see the relevance of the integration up to the exit coordinate. For low fields the 1D description using Eq. (A1) is not accurate.

The region of applicability of the Tong-Lin factor with respect to the laser field can be deduced from Fig. 7, where the exact numerical solution for the ionization rate of hydrogen of Ref. [66] is compared with the Tong-Lin factor. The Tong-Lin factor is reliable up to $E_0 \lesssim 0.15$ a.u.

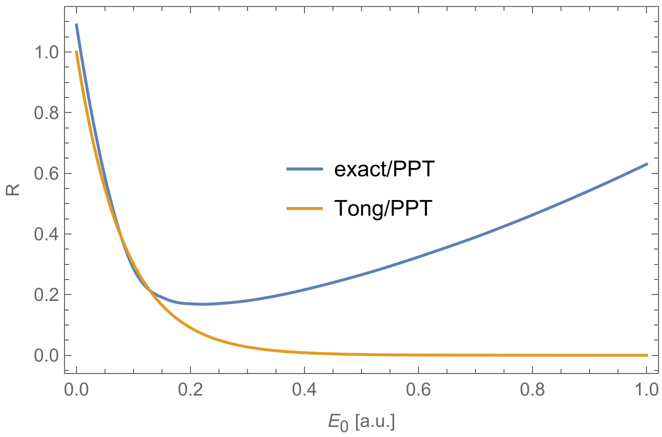

FIG. 7. The ratio $w/w_{\rm PPT}$ for the ionization of hydrogen from the numerical solution in Ref. [66] (blue line) and the Tong-Lin factor from Ref. [34] (orange line).

APPENDIX B: RELATION BETWEEN THE RELATIVISTIC AND NONRELATIVISTIC IONIZATION RATES

In the PPT theory the relativistic rate can be obtained with a correction factor from the nonrelativistic rate [19]:

$$w_{\rm PPT}^{\rm rel} = c^{\rm rel} w_{\rm PPT}^{\rm nr}, \tag{B1}$$

where the correction factor $c^{\rm rel}$ is different for the Dirac and Klein-Gordon equations:

$$c^{\rm rel} = (2\kappa x_s)^{-\mu 2I_p/c^2} \exp\left[\frac{\kappa^2}{36c^2}\frac{E_a}{E_0}\right], \tag{B2}$$

with $\mu = 1$ for the Dirac equation, $\mu = 2$ for the Klein-Gordon equation, and $x_s \approx 2\sqrt{\kappa/E_0}$.

APPENDIX C: ESTIMATION OF THE INTEGRATED-ELECTRON-ENERGY YIELD

We provide the correction to the estimation of the experimental results using the theoretical method in this paper. First of all, we calculate for arbitrary field strength, the quasistatic relativistic correction factor to the PPT rate, according to the model given in this paper:

$$c^{\rm rel}(E_0) = \frac{w^{\rm rel}(E_0)}{w_{\rm PPT}^{\rm rel}(E_0)}. \tag{C1}$$

We use $\kappa = 9.3$ a.u. and $Z \approx 9.3$ a.u., corresponding to the K shell of neon, and a laser field

$$E(t) = E_0 f(t)\cos(\omega t), \tag{C2}$$

with the envelope $f(t) = \cos(\omega t/50)^2$. With the given correction factor, the quasistatic instantaneous ionization rate reads

$$\frac{dw}{dt} = c^{\rm rel}[E_0 f(t)]\sqrt{\frac{3}{\pi}}\sqrt{\frac{E_0 f(t)}{\kappa^3}}\frac{E_0 f(t)}{2\kappa} \times \frac{8\kappa^6}{E_0^2 f(t)^2}\exp\left[-\frac{2\kappa^3}{3E_0 f(t)}\right]. \tag{C3}$$

With the classical mapping of the ionization time t to the final photoelectron energy ε at a given observation angle θ, the integrated electron energy (IEE) is derived via the ionization rate:

$$\frac{d\mathcal{E}(\varepsilon)}{d\Omega} = \int_{E_0}^{\varepsilon} d\varepsilon\varepsilon\frac{dw}{d\varepsilon d\Omega}, \tag{C4}$$

with E_0 being the low cutoff energy corresponding to the applied shield and $d\Omega$ being the solid angle. As the PPT rate is corrected with the factor $c^{\rm rel}$, the IEE is also corrected,

$$\frac{d\mathcal{E}(\varepsilon)}{d\Omega} = c^{\rm rel}[E_0 f(t)]\int_{E_0}^{\varepsilon} d\varepsilon\varepsilon\frac{dw_{\rm PPT}}{d\varepsilon d\Omega}. \tag{C5}$$

We can take into account the depletion effect of the atomic state, which is neglected in the theoretical estimation of Ref. [56]. To this end, we calculate the ionization yield:

$$Y(t) = 1 - \exp\left[-\int_{t^a}^{t} dt'\frac{dw}{dt'}\right], \tag{C6}$$

with $t^a = -25\pi/\omega$. Due to the depletion, the ionization yield is saturated at $t = t_d$, which is determined from the condition

$$\ddot{Y}(t_d) = 0. \tag{C7}$$

Thus, the saturation induces an effective ionization instant t_d, and the IEE is modified due to the depletion effect,

$$\frac{d\mathcal{E}(\varepsilon)}{d\Omega} = c^{\rm rel}[E_0 f(t_d)]\int_{E_0}^{\varepsilon} d\varepsilon\varepsilon\frac{dw_{\rm PPT}}{d\varepsilon d\Omega}[E_0 f(t_d)]. \tag{C8}$$

Figure 5 shows the modified IEE according to the formula above.

APPENDIX D: GAUGE INVARIANCE

In the main text, the length gauge is used for the laser field in the nonrelativistic regime, and its analog, the Göppert-Mayer gauge, is used for the relativistic case. While it is known that the standard SFA is gauge dependent [73–76], the theory developed in this paper is gauge invariant because it accounts for the bound-state dynamics in the laser field.

Let us briefly discuss the role of the gauge for the applied theory. To this end, we present the results of the theory in the velocity gauge. First, we consider the simplest case of the nonrelativistic regime with a 1D zero-range atomic potential. In the velocity gauge $A(t) = E_0 t$, and the Volkov-state reads

$$\psi_0^f = \exp\left[-iE_0^2 t^3/6\right]/\sqrt{2\pi}. \tag{D1}$$

The bound state is corrected by the eikonal in the laser field using the solution of the following equation:

$$-\partial S_1^a = \left(\partial_x S_1^a + E_0 t\right)\partial_x S_0^a - i\partial_{xx}S_1^a/2, \tag{D2}$$

which yields

$$S_1^a = -E_0 tx - iE_0 x^2/2\kappa - iE_0 x/2\kappa^2. \tag{D3}$$

Note the difference in S_1^a above from the length-gauge result in Eq. (22) by the term $-E_0 tx$, which is now missing in the Volkov state [compare Eq. (D1) with (10)]. Further, the atomic correction to the Volkov state is identical to the length gauge.

Consequently, the overlap integral of the corrected bound and Volkov states is the same in the length and velocity gauges. The equation that defines the matching time t^* at which the overlap integral is evaluated is accordingly given by $\partial_t(S_0^a + S_1^a) = \partial_t(S_0^f)$, yielding the same expression as in length gauge. Note S_1^f is time independent in a quasistatic laser field and a zero-range potential. Thus, the results of the length and velocity gauges coincide.

In the nonrelativistic 3D Coulomb case the situation is similar: the atomic eikonal equation in the leading order is

$$-\partial_t S_1^a = \left(\nabla S_1^a + \mathbf{E}_0 t\right)\cdot\nabla S_0^a - i\Delta S_1^a/2, \tag{D4}$$

with the solution

$$S_1^a(x,t) = -E_0 t x - i\kappa x(2+r\kappa)\frac{E_0}{E_a}. \tag{D5}$$

Again, the first term is identical to the one that is missing in the Volkov state in the velocity gauge.

Similarly, one can show in the relativistic case that the four standard gauges, the length, Power-Zienau, Göppert-Mayer, and velocity gauges, with their Volkov states

$$\begin{aligned} \mathcal{S}_0^{f,L} &\sim E_0 t x, \quad \mathcal{S}_0^{f,\mathrm{PZ}} \sim E_0(t - z/2c)x, \\ \mathcal{S}_0^{f,\mathrm{GM}} &\sim E_0(t - z/c)x, \quad \mathcal{S}_0^{f,V} \sim 0, \end{aligned} \tag{D6}$$

give identical results; i.e., the atomic eikonal given in Eq. (55) for the Göppert-Mayer gauge has to be corrected by the difference in the exponents to the Göppert-Mayer eikonal:

$$\mathcal{S}_1^{a,i} = \mathcal{S}_1^{a,\mathrm{GM}} + \left(\mathcal{S}_0^{f,i} - \mathcal{S}_0^{f,\mathrm{GM}}\right). \tag{D7}$$

Thus, the applied theory is gauge invariant.

[1] C. I. Moore, A. Ting, S. J. McNaught, J. Qiu, H. R. Burris, and P. Sprangle, A laser-accelerator injector based on laser ionization and ponderomotive acceleration of electrons, Phys. Rev. Lett. **82**, 1688 (1999).

[2] E. A. Chowdhury, C. P. J. Barty, and B. C. Walker, "Nonrelativistic" ionization of the *L*-shell states in argon by a "relativistic" 10^{19} W/cm^2 laser field, Phys. Rev. A **63**, 042712 (2001).

[3] M. Dammasch, M. Dörr, U. Eichmann, E. Lenz, and W. Sandner, Relativistic laser-field-drift suppression of nonsequential multiple ionization, Phys. Rev. A **64**, 061402(R) (2001).

[4] K. Yamakawa, Y. Akahane, Y. Fukuda, M. Aoyama, N. Inoue, and H. Ueda, Ionization of many-electron atoms by ultrafast laser pulses with peak intensities greater than 10^{19} W/cm^2, Phys. Rev. A **68**, 065403 (2003).

[5] A. Maltsev and T. Ditmire, Above threshold ionization in tightly focused, strongly relativistic laser fields, Phys. Rev. Lett. **90**, 053002 (2003).

[6] E. Gubbini, U. Eichmann, M. Kalashnikov, and W. Sandner, Core relaxation in atomic ultrastrong laser field ionization, Phys. Rev. Lett. **94**, 053602 (2005).

[7] A. D. DiChiara, I. Ghebregziabher, R. Sauer, J. Waesche, S. Palaniyappan, B. L. Wen, and B. C. Walker, Relativistic MeV photoelectrons from the single atom response of argon to a 10^{19} W/cm^2 laser field, Phys. Rev. Lett. **101**, 173002 (2008).

[8] S. Palaniyappan, R. Mitchell, R. Sauer, I. Ghebregziabher, S. L. White, M. F. Decamp, and B. C. Walker, Ionization of methane in strong and ultrastrong relativistic fields, Phys. Rev. Lett. **100**, 183001 (2008).

[9] N. Ekanayake, S. Luo, P. D. Grugan, W. B. Crosby, A. D. Camilo, C. V. McCowan, R. Scalzi, A. Tramontozzi, L. E. Howard, S. J. Wells, C. Mancuso, T. Stanev, M. F. Decamp, and B. C. Walker, Electron shell ionization of atoms with classical, relativistic scattering, Phys. Rev. Lett. **110**, 203003 (2013).

[10] J. W. Yoon, Y. G. Kim, I. W. Choi, J. H. Sung, H. W. Lee, S. K. Lee, and C. H. Nam, Realization of laser intensity over 10^{23} W/cm^2, Optica **8**, 630 (2021).

[11] B. M. Smirnov and M. I. Chibisov, The breaking up of atomic particles by an electric field and by electron collisions, J. Exptl. Theoret. Phys. (U.S.S.R.) **49**, 841 (1965) [Sov. Phys. JETP **22**, 585 (1966)].

[12] A. M. Perelomov and V. S. Popov, Ionization of atoms in an alternating electric field, Zh. Exp. Theor. Fiz. **50**, 1393 (1966) [Sov. Phys. JETP **23**, 924 (1966)].

[13] V. S. Popov, V. P. Kuznetsov, and A. M. Perelomov, Quasiclassical approximation for nonstationary problems, Zh. Eksp. Teor. Fiz. **53**, 331 (1967) [Sov. Phys. JETP **26**, 222 (1968)].

[14] A. M. Perelomov and V. S. Popov, Ionization of atoms in an alternating electric field. III, Zh. Eksp. Teor. Fiz. **52**, 514 (1967) [Sov. Phys. JETP **25**, 336 (1967)].

[15] M. V. Ammosov, N. B. Delone, and V. P. Krainov, Tunnel ionization of complex atoms and of atomic ions in an alternating electromagnetic field, Zh. Eksp. Teor. Fiz. **91**, 2008 (1986).

[16] V. S. Popov, Tunnel and multiphoton ionization of atoms and ions in a strong laser field (Keldysh theory), Phys. Usp. **47**, 855 (2004).

[17] V. Popov, V. Mur, and B. Karnakov, The imaginary-time method for relativistic problems, JETP Lett. **66**, 229 (1997).

[18] V. Mur, B. Karnakov, and V. Popov, Relativistic version of the imaginary-time formalism, J. Exp. Theor. Phys. **87**, 433 (1998).

[19] N. Milosevic, V. P. Krainov, and T. Brabec, Semiclassical Dirac theory of tunnel ionization, Phys. Rev. Lett. **89**, 193001 (2002).

[20] N. Milosevic, V. P. Krainov, and T. Brabec, Relativistic theory of tunnel ionization, J. Phys. B **35**, 3515 (2002).

[21] S. V. Popruzhenko, Relativistic tunneling ionization in crossed petawatt laser beams, JETP Lett. **117**, 281 (2023).

[22] S. V. Popruzhenko, Relativistic tunneling effect under ionization of multiply charged ions in multi-petawatt laser beams, Bull. Lebedev Phys. Inst. **50**, S928 (2023).

[23] L. V. Keldysh, Ionization in the field of a strong electromagnetic wave, Zh. Eksp. Teor. Fiz. **47**, 1945 (1964) [Sov. Phys. JETP **20**, 1307 (1965)].

[24] F. H. M. Faisal, Multiple absorption of laser photons by atoms, J. Phys. B **6**, L89 (1973).

[25] H. R. Reiss, Effect of an intense electromagnetic field on a weakly bound system, Phys. Rev. A **22**, 1786 (1980).

[26] H. R. Reiss, Complete Keldysh theory and its limiting cases, Phys. Rev. A **42**, 1476 (1990).

[27] H. R. Reiss, Relativistic strong-field photoionization, J. Opt. Soc. Am. B **7**, 574 (1990).

[28] H. G. Hetzheim and C. H. Keitel, Ionization dynamics versus laser intensity in laser-driven multiply charged ions, Phys. Rev. Lett. **102**, 083003 (2009).

[29] H. Bauke, H. G. Hetzheim, G. R. Mocken, M. Ruf, and C. H. Keitel, Relativistic ionization characteristics of laser-driven hydrogenlike ions, Phys. Rev. A **83**, 063414 (2011).

[30] M. F. Ciappina, S. V. Popruzhenko, S. V. Bulanov, T. Ditmire, G. Korn, and S. Weber, Progress toward atomic diagnostics of ultrahigh laser intensities, Phys. Rev. A **99**, 043405 (2019).

[31] M. F. Ciappina and S. V. Popruzhenko, Diagnostics of ultra-intense laser pulses using tunneling ionization, Laser Phys. Lett. **17**, 025301 (2020).

[32] A. Scrinzi, M. Geissler, and T. Brabec, Ionization above the Coulomb barrier, Phys. Rev. Lett. **83**, 706 (1999).

[33] D. Bauer and P. Mulser, Exact field ionization rates in the barrier-suppression regime from numerical time-dependent Schrödinger-equation calculations, Phys. Rev. A **59**, 569 (1999).

[34] X. M. Tong and C. D. Lin, Empirical formula for static field ionization rates of atoms and molecules by lasers in the barrier-suppression regime, J. Phys. B **38**, 2593 (2005).

[35] E. Lötstedt, M. F. Ciappina, and K. Yamanouchi, Static-field ionization model of He-like ions for diagnostics of light-field intensity, Phys. Rev. A **102**, 013112 (2020).

[36] E. C. Jones, Z. P. Andreula, and B. C. Walker, Polarizability, Stark shifts, and field ionization of highly charged ions in ultraintense lasers, Phys. Rev. A **107**, 033102 (2023).

[37] P. A. Batishchev, O. I. Tolstikhin, and T. Morishita, Atomic Siegert states in an electric field: Transverse momentum distribution of the ionized electrons, Phys. Rev. A **82**, 023416 (2010).

[38] O. I. Tolstikhin, T. Morishita, and S. Watanabe, Adiabatic theory of ionization of atoms by intense laser pulses: One-dimensional zero-range-potential model, Phys. Rev. A **81**, 033415 (2010).

[39] O. I. Tolstikhin and T. Morishita, Adiabatic theory of ionization by intense laser pulses: Finite-range potentials, Phys. Rev. A **86**, 043417 (2012).

[40] V. H. Trinh, O. I. Tolstikhin, L. B. Madsen, and T. Morishita, First-order correction terms in the weak-field asymptotic theory of tunneling ionization, Phys. Rev. A **87**, 043426 (2013).

[41] S. X. Hu and C. H. Keitel, Spin signatures in intense laser-ion interaction, Phys. Rev. Lett. **83**, 4709 (1999).

[42] M. Casu, C. Szymanowski, S. Hu, and C. H. Keitel, Coherent x-ray generation with laser driven ions, J. Phys. B **33**, L411 (2000).

[43] C. H. Keitel and S. X. Hu, Coherent x-ray pulse generation in the sub-Ångström regime, Appl. Phys. Lett. **80**, 541 (2002).

[44] M. W. Walser, D. J. Urbach, K. Z. Hatsagortsyan, S. X. Hu, and C. H. Keitel, Spin and radiation in intense laser fields, Phys. Rev. A **65**, 043410 (2002).

[45] G. R. Mocken and C. H. Keitel, Bound atomic dynamics in the MeV regime, J. Phys. B **37**, L275 (2004).

[46] G. Mocken and C. H. Keitel, FFT-split-operator code for solving the Dirac equation in 2+1 dimensions, Comput. Phys. Commun. **178**, 868 (2008).

[47] S. Selstø, E. Lindroth, and J. Bengtsson, Solution of the Dirac equation for hydrogenlike systems exposed to intense electromagnetic pulses, Phys. Rev. A **79**, 043418 (2009).

[48] Y. V. Vanne and A. Saenz, Solution of the time-dependent Dirac equation for multiphoton ionization of highly charged hydrogenlike ions, Phys. Rev. A **85**, 033411 (2012).

[49] F. Fillion-Gourdeau, E. Lorin, and A. D. Bandrauk, Numerical solution of the time-dependent Dirac equation in coordinate space without fermion-doubling, Comput. Phys. Commun. **183**, 1403 (2012).

[50] T. Kjellsson, S. Selstø, and E. Lindroth, Relativistic ionization dynamics for a hydrogen atom exposed to superintense XUV laser pulses, Phys. Rev. A **95**, 043403 (2017).

[51] D. A. Telnov and S.-I. Chu, Relativistic ionization dynamics of hydrogenlike ions in strong electromagnetic fields: Generalized pseudospectral method for the time-dependent Dirac equation, Phys. Rev. A **102**, 063109 (2020).

[52] B. Hafizi, D. F. Gordon, and J. P. Palastro, First benchmark of relativistic photoionization theories against 3D *ab initio* simulation, Phys. Rev. Lett. **118**, 133201 (2017).

[53] J. Z. Kamiński, Eikonal approximation to potential free-free transition, Acta Phys. Pol. A **66**, 517 (1984).

[54] H. K. Avetissian, K. Z. Hatsagortsian, A. G. Markossian, and S. V. Movsissian, Generalized eikonal wave function of a Dirac particle interacting with an arbitrary potential and radiation fields, Phys. Rev. A **59**, 549 (1999).

[55] F. Cajiao Vélez, K. Krajewska, and J. Z. Kamiński, Generalized eikonal approximation for strong-field ionization, Phys. Rev. A **91**, 053417 (2015).

[56] A. Yandow, T. N. Ha, C. Aniculaesei, H. L. Smith, C. G. Richmond, M. M. Spinks, H. J. Quevedo, S. Bruce, M. Darilek, C. Chang, D. A. Garcia, E. Gaul, M. E. Donovan, B. M. Hegelich, and T. Ditmire, Above-threshold ionization at laser intensity greater than 10^{20} W/cm^2, Phys. Rev. A **109**, 023119 (2024).

[57] L. D. Landau and E. M. Lifshitz, *Quantum Mechanics* (Pergamon, Oxford, 1977), Chap. 53, p. 293.

[58] A. M. Dykhne, Adiabatic perturbation TOF discrete spectrum states, Sov. Phys. JETP **14**, 941 (1962).

[59] J. S. Briggs, V. I. Savichev, and E. A. Solov'ev, Hidden crossings and excitation of hydrogen by a slow electric pulse, J. Phys. B **33**, 3363 (2000).

[60] D. Dimitrovski, T. P. Grozdanov, E. A. Solovev, and J. S. Briggs, Ionization and excitation of the hydrogen atom by an electric pulse, J. Phys. B **36**, 1351 (2003).

[61] M. Klaiber, J. Daněk, E. Yakaboylu, K. Z. Hatsagortsyan, and C. H. Keitel, Strong-field ionization via a high-order Coulomb-corrected strong-field approximation, Phys. Rev. A **95**, 023403 (2017).

[62] W. Becker, F. Grasbon, R. Kopold, D. B. Milošević, G. G. Paulus, and H. Walther, Above-threshold ionization: From classical features to quantum effects, Adv. At. Mol. Opt. Phys. **48**, 35 (2002).

[63] H. A. Bethe and E. E. Salpeter, *Quantum Mechanics of One- and Two-Electron Atoms* (Academic Press, New York, 1957).

[64] M. H. Alexander, Exact treatment of the Stark effect in atomic hydrogen, Phys. Rev. **178**, 34 (1969).

[65] R. J. Damburg and V. V. Kolosov, An asymptotic approach to the Stark effect for the hydrogen atom, J. Phys. B **11**, 1921 (1978).

[66] C. A. Nicolaides and S. I. Themelis, Theory of the resonances of the Losurdo-Stark effect, Phys. Rev. A **45**, 349 (1992).

[67] U. D. Jentschura, Resummation of the divergent perturbation series for a hydrogen atom in an electric field, Phys. Rev. A **64**, 013403 (2001).

[68] D. M. Wolkow, On a class of solutions of the Dirac equation, Z. Phys. **94**, 250 (1935).
[69] M. Klaiber, E. Yakaboylu, and K. Z. Hatsagortsyan, Above-threshold ionization with highly charged ions in superstrong laser fields. II. Relativistic coulomb-corrected strong-field approximation, Phys. Rev. A **87**, 023418 (2013).
[70] M. Klaiber, E. Yakaboylu, H. Bauke, K. Z. Hatsagortsyan, and C. H. Keitel, Under-the-barrier dynamics in laser-induced relativistic tunneling, Phys. Rev. Lett. **110**, 153004 (2013).
[71] S. Augst, D. D. Meyerhofer, D. Strickland, and S. L. Chin, Laser ionization of noble gases by Coulomb-barrier suppression, J. Opt. Soc. Am. B **8**, 858 (1991).
[72] M. Klaiber, K. Z. Hatsagortsyan, and C. H. Keitel, Relativistic analytical R-matrix theory for strong-field ionization, Phys. Rev. A **107**, 023107 (2023).
[73] M. Klaiber, K. Z. Hatsagortsyan, and C. H. Keitel, Gauge-invariant relativistic strong-field approximation, Phys. Rev. A **73**, 053411 (2006).
[74] F. H. M. Faisal, Gauge-invariant intense-field approximations to all orders, J. Phys. B **40**, F145 (2007).
[75] F. H. M. Faisal, Gauge-equivalent intense-field approximations in velocity and length gauges to all orders, Phys. Rev. A **75**, 063412 (2007).
[76] H. R. Reiss, Velocity-gauge theory for the treatment of strong-field photodetachment, Phys. Rev. A **76**, 033404 (2007).